DALTON
FULL PAPER

Chelating *versus* bridging behaviour and NMR fluxionality of dppf in the *nido* clusters $[M_3Se_2(CO)_7(dppf)]$ [M = Fe or Ru, dppf = $Fe(\eta^5\text{-}C_5H_4PPh_2)_2$]. Crystal structure of the chelated ruthenium derivative †

Daniele Cauzzi,[a] Claudia Graiff,[a] Chiara Massera,[a] Giovanni Predieri,*[a] Antonio Tiripicchio[a] and Domenico Acquotti[b]

[a] *Dipartimento di Chimica Generale ed Inorganica, Chimica Analitica, Chimica Fisica, Università di Parma, Centro di Studio per la Strutturistica Diffrattometrica del CNR, Parco Area delle Scienze, I-43100 Parma, Italy. E-mail: predieri@ipruniv.cce.unipr.it*
[b] *Centro Interfacoltà di Misure 'Giuseppe Casnati', Università di Parma, Parco Area delle Scienze, I-43100 Parma, Italy*

Received 18th June 1999, Accepted 5th August 1999

The reactions of $[M_3(CO)_{12}]$ (M = Fe or Ru) with the diphosphine diselenide $dppfSe_2$ [$dppfSe_2 = Fe(\eta^5\text{-}C_5H_4P(Ph_2)\text{-}Se)_2$], in the presence of Me_3NO afforded the disubstituted square pyramidal selenido clusters $[Fe_3Se_2(CO)_7(\mu\text{-dppf})]$ **1** and $[Ru_3Se_2(CO)_7(dppf)]$ **2**. In the previously reported structure of **1** the dppf ligand bridges the two non-bonded iron atoms, whereas in **2** the same ligand chelates to one ruthenium atom of the basal plane of the square pyramidal cluster. Compound **2** represents the first reported example of chelating dppf to a carbonyl cluster. Both compounds exhibit fluxional behaviour in solution, consisting in the rocking motion of the bidentate bridging ligand below the square basal plane of the iron clusters in **1** and in the exchange of the axial and equatorial positions between the two chelating P atoms in **2**. The dynamic behaviour of both compounds was studied by variable temperature 1-D and 2-D COSY and EXSY ^{1}H NMR. The solid state structures correspond to the static structures in solution below 258 K for **1** and 213 K for **2**. The cluster $[Ru_3Se_2(CO)_7(\mu\text{-dppe})]$ **3** [dppe = $(CH_2PPh_2)_2$] has also been synthesized from $dppeSe_2$, and its structure determined for comparison.

Introduction

Among the methods for the synthesis of transition-metal clusters containing bridging chalcogenido ligands,[1] that involving tertiary phosphine chalcogenide R_3PE (E = S, Se or Te) has been proved to be one of the most effective.[2–6] This method takes advantage of the frailty of the P=E bond, which leads to the production of phosphine-substituted chalcogenido clusters through oxidative transfer of chalcogen atoms to zero-valent metal complexes.

As regards chelating diphosphines, we have recently found that the reactions of $[Fe_3(CO)_{12}]$ with three diphosphine diselenides $dppmSe_2$, $dppeSe_2$, $dppfSe_2$ produce the substituted 50-electron, *nido*-clusters $[Fe_3(\mu_3\text{-}Se)_2(CO)_7\{\mu\text{-}(Ph_2P)_2R\}]$ (R = CH_2, dppm; R = $(CH_2)_2$, dppe; R = $(C_5H_4)_2Fe$, dppf) as the main products.[7] These carbonyl clusters have a square-pyramidal Fe_3Se_2 core with two iron and two selenium atoms alternating in the basal plane and the third iron atom at the apex of the pyramid. The phosphorus substitution appears regioselective for the M_3E_2 (E = chalcogen element) clusters,[8,9] occurring preferentially on the two basal metal atoms, in such a way that the diphosphines act as bridging ligands between them as shown for the iron selenido clusters.

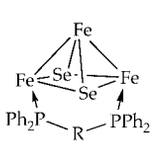

R = CH_2 dppm
R = CH_2CH_2 dppe
R = $Fe(C_5H_4)_2$ dppf

$[Fe_3(\mu_3\text{-}Se)_2(CO)_7\{\mu\text{-}(Ph_2P)_2R\}]$

† *Supplementary data available*: rotatable 3-D crystal structure diagram in CHIME format. See http://www.rsc.org/suppdata/dt/1999/3515/

Considering the ruthenium species, we have observed[10] that the diphosphine diselenide $(Ph_2PSe)_2CH_2$ ($dppmSe_2$) reacts in toluene with $[Ru_3(CO)_{12}]$ to give the *nido*-cluster $[Ru_3(\mu_3\text{-}Se)_2(CO)_7(\mu\text{-dppm})]$ (the expected primary product), the *closo*-octahedral species $[Ru_4(\mu_4\text{-}Se)_2(CO)_9(dppm)]$ and $[Ru_4(\mu_3\text{-}Se)_4(CO)_{10}(dppm)]$ (dppm = $(Ph_2P)_2CH_2$), which is the first reported 72-electron Ru–Se cubane-like cage complex.[10a]

In order to compare the behaviour of ruthenium and iron carbonyls towards diphosphine diselenides, we have treated $[Ru_3(CO)_{12}]$ with $dppfSe_2$ and $dppeSe_2$, in the presence of Me_3NO, obtaining the *nido*-clusters $[Ru_3(\mu_3\text{-}Se)_2(CO)_7(dppf)]$ **2** and $[Ru_3(\mu_3\text{-}Se)_2(CO)_7(\mu\text{-dppe})]$ **3**, respectively. The main result of this work is the achievement of the first metal carbonyl cluster containing chelating dppf, consequently the first part of the discussion will regard the description of the crystal structure of **2**, in comparison with that of the corresponding iron cluster $[Fe_3(\mu_3\text{-}Se)_2(CO)_7(\mu\text{-dppf})]$ **1**. The second part will deal with the dynamic behaviour in solution of **1** and **2**. Two recent reviews by Gan and Hor[11a] and Zanello,[11b] regarding the structural and chemical aspects of metal complexes of dppf and related ligands, and the files of the Cambridge Structural Database[12] have furnished the grounds for this discussion.

Experimental

General

The starting reagents $[Fe_3(CO)_{12}]$, $[Ru_3(CO)_{12}]$, KNCSe and the diphosphines $(Ph_2P)_2R$ (R = $(C_5H_4)_2Fe$, dppf; R = CH_2CH_2, dppe) were pure commercial products (Aldrich and Fluka) used as received. The solvents (C. Erba) were dried and distilled by standard techniques before use. All manipulations (prior to the TLC separations) were carried out under dry nitrogen by

means of standard Schlenk-tube techniques. Elemental (C, H) analyses were performed with a Carlo Erba EA 1108 automated analyser. The IR spectra (KBr discs or CH_2Cl_2 solutions) were recorded on a Nicolet 5PC FT spectrometer.

NMR Measurements were performed on $CDCl_3$ solutions in standard 5 mm tubes. A Eurotherm B-VT2000 variable-temperature equipment was used to control the probe temperature with accuracy of ±1 °C. The ^{1}H NMR, COSY, EXSY and ROESY (rotating frame Overhauser enhancement spectroscopy) spectra of clusters were recorded on a Bruker AMX 400 spectrometer operating at 400.13 MHz using $SiMe_4$ as internal reference: EXSY spectra were taken with a mixing time variable in the range of 0.3–0.7 s, ROESY spectra with spin-lock times of 120 and 160 ms. The ^{31}P (81.0 MHz) and ^{77}Se (38.2 MHz) NMR spectra were recorded on a Bruker CXP 200 instrument; external references were 85% H_3PO_4(aq) and Ph_2Se_2 in $CHCl_3$ (δ +461 relative to Me_2Se), respectively.

Syntheses

Diphosphine diselenides and cluster 1. The reagents $dppfSe_2$ and $dppeSe_2$ were prepared according to literature methods by selenium transfer from KSeCN to the corresponding diphosphines.[7] The compound $[Fe_3Se_2(CO)_7(\mu\text{-dppf})]$ **1** was synthesized by reaction of $[Fe_3(CO)_{12}]$ with $dppfSe_2$, as previously described.[7] Cluster **1**·CH_2Cl_2: ^{1}H NMR (258 K, $CDCl_3$) δ 8.04 (s, 4 H, Ph), 7.58 (s, 6 H, Ph), 7.26 (s, 6 H, Ph), 7.03 (s, 4 H, Ph), 5.31 (s, 2 H, CH_2Cl_2), 4.75, 4.24, 4.01, 3.46 (s, 2 H each; protons *a*, *b*, *c*, *d* respectively, Scheme 3).

Cluster 2. Treatment of $[Ru_3(CO)_{12}]$ (152 mg, 0.24 mmol) with 170 mg of $dppfSe_2$ (0.24 mmol) and 18 mg of Me_3NO for 1.5 h in toluene, at 70 °C, under N_2, gave a deep brown solution, which was evaporated to dryness and the residue redissolved in a small amount of CH_2Cl_2. TLC Separation on silica, using dichloromethane–light petroleum (bp 50–70 °C) (2 : 1) as eluent, yielded an orange band, a red one and some decomposition. The orange band contains $[Ru_3(\mu_3\text{-}Se)_2(CO)_7(dppf)]$ **2** as the major component (30%) and minor amounts of a product exhibiting a ^{31}P resonance at δ 53.8. The product corresponding to the red band is under investigation. Purification by crystallization (from a CH_2Cl_2–MeOH mixture at 5 °C for some days) of the major product of the orange band gave well formed crystals of **2**, as the dichloromethane solvate (**2**·CH_2Cl_2), suitable for X-ray analysis (Found: C, 39.9; H, 2.5. Calc. for $C_{41}H_{28}FeO_7P_2Ru_3Se_2$: C, 40.6; H, 2.33%). IR (CH_2Cl_2, ν(CO), cm^{-1}): 2067, 2052, 2034, 2020, 1986 and 1933. ^{1}H NMR (213 K, $CDCl_3$): δ 4.94, 4.84, 4.49, 4.31, 4.13, 4.10, 4.05, 3.67 (s, 1 H each, protons *a*, *a*′, *b*, *b*′, *c*, *c*′, *d*, *d*′ respectively); (297 K) 4.73, 4.34, 4.11, 3.97 (s, 2 H each). ^{31}P NMR (213 K, $CDCl_3$): δ 57.4 (d, axial P) and 40.2 (d, equatorial P).

Cluster 3. Treatment of $[Ru_3(CO)_{12}]$ (172 mg, 0.26 mmol) with 150 mg of $dppeSe_2$ (0.26 mmol) and 20 mg of Me_3NO for 1.5 h in toluene, at 70 °C, under N_2, gave a deep brown solution, which, upon TLC purification, yielded orange $[Ru_3(\mu_3\text{-}Se)_2(CO)_7(dppe)]$ **3** (40%) and decomposition products. Crystallization of **3** (from a CH_2Cl_2–MeOH mixture at 5 °C for some days) afforded crystals suitable for X-ray analysis. IR (CH_2Cl_2, ν(CO), cm^{-1}): 2066(sh), 2050, 2016 and 1976. ^{1}H NMR ($CDCl_3$): δ 2.68 (d, 4 H, CH_2, J(H,P) 7 Hz). ^{31}P NMR ($CDCl_3$): δ 57.3 (s). ^{77}Se NMR ($CDCl_3$): δ −231 (t, J(Se,P) 10 Hz).

X-Ray data collection, structure solution and refinement for $[Ru_3(\mu_3\text{-}Se)_2(CO)_7(dppf)]\cdot CH_2Cl_2$ (**2**·CH_2Cl_2) and $[Ru_3(\mu_3\text{-}Se)_2(CO)_7(dppe)]$ **3**

The crystallographic data for the compounds **2**·CH_2Cl_2 and **3** are summarized in Table 1. Intensities were corrected for Lorentz-polarization effects and for absorption [maximum and minimum value transmission coefficient 1 and 0.9026 for **3** and 1 and 0.8196 for **2**·CH_2Cl_2].[13]

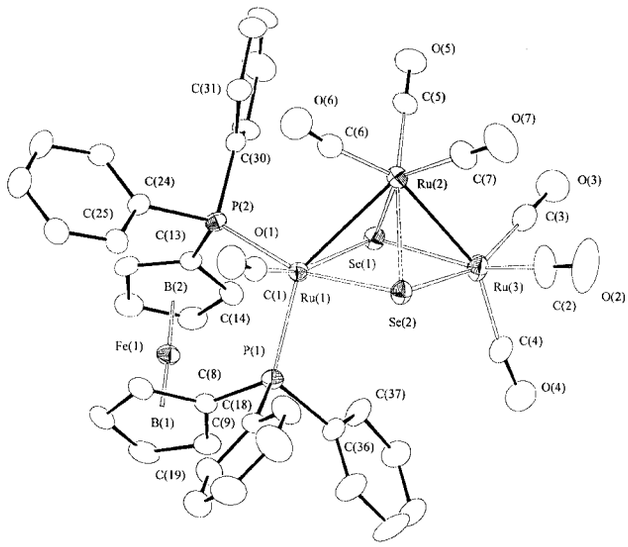

Fig. 1 Perspective view of the molecular structure of the cluster $[Ru_3Se_2(CO)_7(dppf)]$ **2**. The thermal ellipsoids are drawn at the 30% probability level; B(1) and B(2) indicate the centroids of the cyclopentadienyl rings.

Both structures were solved by Patterson methods using SHELXS 86[14] and refined by full matrix least-squares procedures (based on F_o^2) using SHELX 97[15] (compound **3**) and SHELXL 93[16] (**2**·CH_2Cl_2), first with isotropic and then with anisotropic thermal parameters for all non-hydrogen atoms. In both structures the hydrogen atoms were placed at their geometrically calculated positions (C–H 0.96 Å) and refined "riding" on the corresponding carbon atoms. All calculations were carried out on the GOULD POWERNODE 6040 and ENCORE 91 computers of the Centro di Studio per la Strutturistica Diffrattometrica del C.N.R., Parma.

CCDC reference number 186/1609.

See http://www.rsc.org/suppdata/dt/1999/3515/ for crystallographic files in .cif format.

Results and discussion

Syntheses and crystal structures

As pointed out in the Introduction, previous investigations showed that the main products of the reaction of $[Fe_3(CO)_{12}]$ with diphosphine diselenides are the substituted open-triangular, *nido*-clusters $[Fe_3(\mu_3\text{-}Se)_2(CO)_7\{\mu\text{-}(Ph_2P)_2R\}]$. In spite of their different bites, all the three diphosphines dppm, dppe and dppf bridge the two non-bonded iron atoms, owing to the inertness of the apical position towards phosphine substitution. This produces a certain degree of deformation in the cluster core Fe_3Se_2, which appears to depend on the P···P span.[7] The short-bite dppm ligand impels the basal iron atoms to approach (3.50 Å), with respect to the distance observed with dppe (3.56 Å, chosen as reference). In this way a fluxional motion takes place in solution consisting of the reversible migration of a metal–metal bond from one side of the open triangle to the basal plane, resulting in linking of the two basal iron atoms.[7] This has recently been observed also for the corresponding ruthenium derivative $[Ru_3(\mu_3\text{-}Se)_2(CO)_7(\mu\text{-dppm})]$.[10b] On the contrary the large bite adopted by the dppf ligand (5.51 Å) forces the basal iron atoms to move slightly away (3.63 Å).

The results of this work indicate that also $[Ru_3(CO)_{12}]$ reacts with dppf and dppe affording respectively the expected *nido* clusters **2** and **3**, as major products. Their molecular structures are shown in Figs. 1 and 2; selected bond distances and angles are given in Tables 2 and 3.

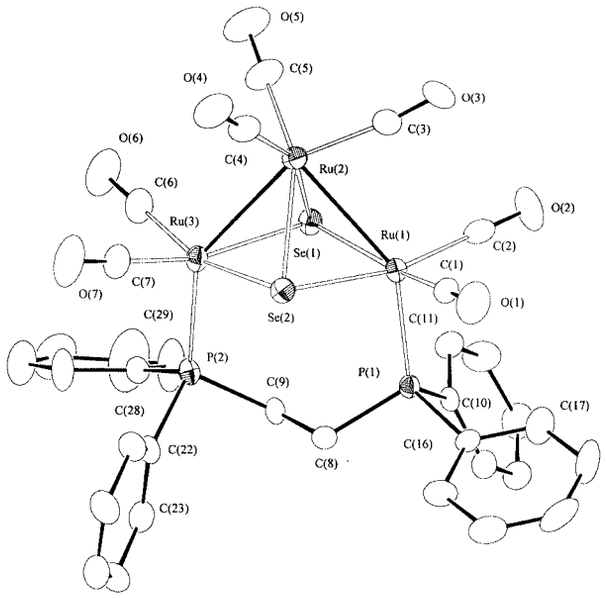

Fig. 2 Perspective view of the molecular structure of the cluster $[Ru_3Se_2(CO)_7(\mu\text{-dppe})]$ **3**. The thermal ellipsoids are drawn at the 30% probability level.

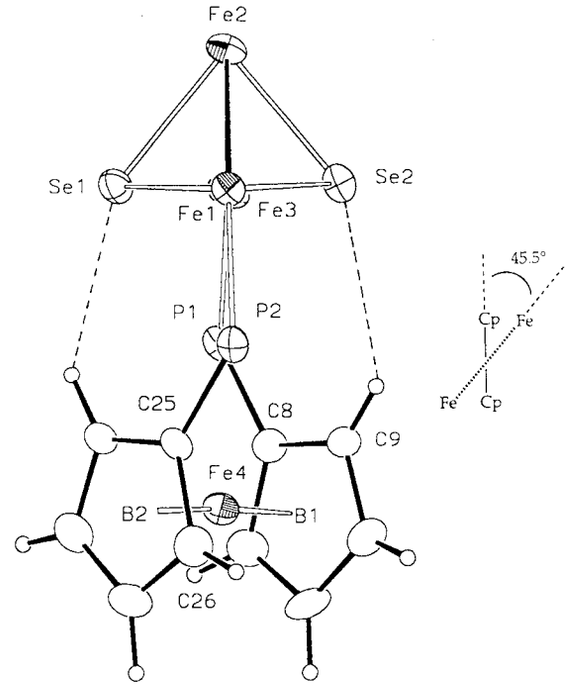

Fig. 3 Perspective view of the molecular structure of the cluster $[Fe_3Se_2(CO)_7(\mu\text{-dppf})]$ **1** (carbonyl ligands and phenyl rings omitted) emphasizing the two H(Cp)···Se interactions: H(29)···Se(1) 2.63(8) Å, C(29)–H(29)···Se(1) 140(6)°; H(9)···Se(2) 2.84(7) Å, C(9)–H(9)···Se(2) 141(6)°; B(1) and B(2) indicate the centroids of the cyclopentadienyl rings.

While dppe behaves as bridging ligand in **3**, unexpectedly dppf prefers to chelate one of the basal ruthenium atoms in **2**. Even if a minor product with a ^{31}P resonance at δ 53.8 has been detected, which could be the bridging Ru_3Se_2/dppf derivative, the achievement of the chelated dppf cluster **2** is quite unexpected, considering that in all the reported dppf-substituted metal carbonyl clusters the bidentate ligand adopts a bridging behaviour both on bonding M–M and on non-bonding M···M sides.[11a]

In particular, focusing attention on the dppf-substituted ruthenium clusters reported,[17–20] the bridging diphosphine ligand exhibits its ability to span a wide range of Ru–Ru distances (2.89–3.14 Å) by varying the P···P separation (5.02–5.44 Å). This ability to fit different co-ordination demands derives from the possibility of the Cp rings to twist about the B1–Fe–B2 axis (B1,2 = Cp centroids, see Figs. 1 and 3).

In fact, if we neglect the possible ring tilts, due to lack of collinearity of the two Fe–B1,2 vectors, and the displacement of P atoms from coplanarity with the Cp rings, the *d*(PP) distance between the two donor atoms depends on the θ torsional angle as shown in Scheme 1. Assuming 3.03 and 3.30 Å as the

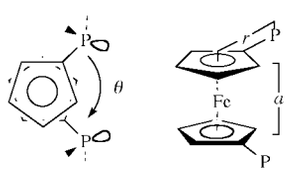

$$d(\mathrm{PP}) = \sqrt{(2\,r\sin\theta/2)^2 + a^2}$$

Scheme 1

mean values of the *r* and *a* segments respectively, the *d* values range from 3.30 ($\theta = 0°$, synperiplanar conformation[11a]) to 6.90 Å ($\theta = 180°$, antiperiplanar). Scheme 2 shows the preferred

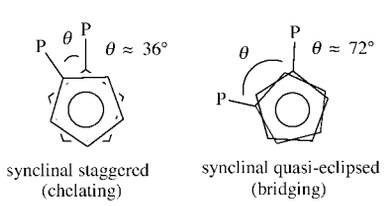

Scheme 2

conformations adopted in the case of chelating behaviour (synclinal staggered) and in the case of bridging behaviour over a side of a metal carbonyl cluster (synclinal eclipsed).

A large M···M separation, as in the case of the basal atoms in the M_3Se_2 *nido* clusters, forces bridging dppf to fit in by increasing the torsional angle θ, causing the Cp moieties to approach the metal cluster. Actually, what happens in the case of the triiron cluster **1** is well illustrated in Fig. 3: the torsional angle θ of 80° (P···P and Fe···Fe separations 5.51 and 3.63 Å respectively) produces a particular arrangement of the various fragments which promotes the two C–H···Se contacts H(29)···Se(1) 2.63(8) and H(9)···Se(2) 2.84(7) Å shown in Fig. 3. These interactions are significantly shorter than the sum of the relevant van der Waals radii (H 1.2, Se 2.0 Å),[21] resembling hydrogen bonds.

In the case of the Ru_3Se_2 *nido* clusters, the longer Ru···Ru basal separation (3.75 in **3**, 3.87 in **2** and 3.84 Å in $[Ru_3Se_2(CO)_7(Ph_3P)_2]$[5]) should require a larger torsional angle θ, probably unsuitable for the formation of the two C–H···Se interactions. By failing these favourable circumstances, the chelating behaviour becomes competitive. Consequently, dppf adopts a synclinal staggered conformation ($\theta = 34.5(2)°$, P···P 3.67 Å) as normally observed in mononuclear ruthenium chelated complexes,[22] with only one exception, $[Ru\{\eta^6\text{-}(p\text{-}MeC_6H_4Pr^i)\}(dppf)Cl]PF_6$, where dppf exhibits a synperiplanar (eclipsed, $\theta = 0°$) geometry.[23]

In cluster **2** the two Ru(1)–P distances are significantly different: (*i*) Ru(1)–P(1) (2.31 Å, axial position, *transoid* to Ru) is shorter and well comparable with those observed in the μ-dppe derivative **3** where dppe bridges, as expected, the two basal ruthenium atoms in the axial positions (Ru–P 2.29 and 2.31 Å); (*ii*) Ru(1)–P(2) (2.37 Å, equatorial, transoid to Se) is longer and equal to the equatorial Ru–P separation observed in $[Ru_3Se_2(CO)_7(Ph_3P)_2]$,[5] suggesting that the Ru–P interaction in the Ru_3Se_2 *nido* clusters could suffer a sort of *trans* effect.

Moreover, the double phosphorus substitution on Ru(1) appears to cause an important deformation in the cluster core, the two Ru–Ru bond lengths being quite different. In fact,

Table 1 Summary of crystallographic data for the compounds **2**·CH_2Cl_2 and **3**

	2·CH_2Cl_2	**3**
Formula	$C_{41}H_{28}FeO_7P_2Ru_3Se_2 \cdot CH_2Cl_2$	$C_{33}H_{24}O_7P_2Ru_3Se_2$
M	1296.52	1055.59
Crystal system	Triclinic	Monoclinic
Space group	$P\bar{1}$	$P2_1/c$
a/Å	9.201(2)	13.550(5)
b/Å	12.020(3)	10.891(4)
c/Å	21.405(5)	24.876(6)
α/°	79.77(2)	—
β/°	84.24(3)	102.31(2)
γ/°	72.31(2)	—
V/Å^3	2217(1)	3587(2)
Z	2	4
T/K	293(2)	293(2)
μ(Mo-Kα)/cm^{-1}	32.06	34.11
Unique total data	10683	8658
Unique observed data	4549 [$I > 2\sigma(I)$]	3277 [$I > 2\sigma(I)$]
$R1$	0.0425 (0.1194 for all data)	0.0543 (0.2953 for all data)
wR	0.1012 (0.1449 for all data)	0.1370 (0.2664 for all data)

Table 2 Selected bond distances (Å) and angles (°) for compound **2**·CH_2Cl_2

Ru(1)–Ru(2)	2.907(1)	Ru(2)–Ru(3)	2.760(1)
Ru(1)–Se(1)	2.501(1)	Ru(1)–Se(2)	2.514(1)
Ru(2)–Se(1)	2.543(1)	Ru(2)–Se(2)	2.522(1)
Ru(3)–Se(1)	2.508(1)	Ru(3)–Se(2)	2.521(1)
Ru(1)–P(1)	2.308(2)	Ru(1)–P(2)	2.368(2)
Fe(1)–B(1)	1.653(7)	Fe(1)–B(2)	1.642(7)
Se(2)–Ru(1)–P(2)	162.6(1)	Se(2)–Ru(1)–P(1)	95.6(1)
Se(1)–Ru(1)–P(2)	89.6(1)	Se(1)–Ru(1)–P(1)	109.7(1)
Se(1)–Ru(1)–Se(2)	79.0(1)	Se(1)–Ru(2)–Se(2)	78.0(1)
Ru(2)–Ru(1)–P(2)	107.8(1)	Ru(2)–Ru(1)–P(1)	147.1(1)
Ru(2)–Ru(1)–Se(2)	54.9(1)	Ru(2)–Ru(1)–Se(1)	55.5(1)
Ru(1)–Ru(2)–Se(2)	54.6(1)	Ru(1)–Ru(2)–Se(1)	54.1(1)
Ru(1)–Ru(2)–Ru(3)	86.2(1)	Se(1)–Ru(3)–Se(2)	78.7(1)
Ru(3)–Ru(2)–Se(2)	56.8(1)	Ru(3)–Ru(2)–Se(1)	56.3(1)
Ru(2)–Ru(3)–Se(2)	56.8(1)	Ru(2)–Ru(3)–Se(1)	57.5(1)
Ru(2)–Se(1)–Ru(3)	66.2(1)	Ru(2)–Se(2)–Ru(3)	66.3(1)
Ru(1)–Se(1)–Ru(3)	101.3(1)	Ru(1)–Se(2)–Ru(3)	100.6(1)
Ru(1)–Se(1)–Ru(2)	70.4(1)	Ru(1)–Se(2)–Ru(2)	70.5(1)
P(1)–Ru(1)–P(2)	100.6(1)	B(1)–Fe(1)–B(2)	178.8(4)

B(1) and B(2) are the centroids of the two cyclopentadienyl rings.

Table 3 Selected bond distances (Å) and angles (°) for compound **3**

Se(1)–Ru(1)	2.504(2)	Se(2)–Ru(1)	2.494(2)
Se(1)–Ru(3)	2.502(2)	Se(2)–Ru(3)	2.492(2)
Se(1)–Ru(2)	2.530(2)	Se(2)–Ru(2)	2.539(2)
Ru(1)–Ru(2)	2.828(2)	Ru(3)–Ru(2)	2.796(2)
Ru(1)–P(1)	2.291(4)	Ru(3)–P(2)	2.310(4)
P(1)–Ru(1)–Se(2)	97.6(1)	P(2)–Ru(3)–Se(2)	98.9(1)
P(1)–Ru(1)–Se(1)	98.7(1)	P(2)–Ru(3)–Se(1)	95.3(1)
Se(2)–Ru(1)–Se(1)	82.12(6)	Se(2)–Ru(3)–Se(1)	82.13(6)
P(1)–Ru(1)–Ru(2)	143.7(1)	P(2)–Ru(3)–Ru(2)	142.9(1)
Se(2)–Ru(1)–Ru(2)	56.57(5)	Se(2)–Ru(3)–Ru(2)	57.03(5)
Se(1)–Ru(1)–Ru(2)	56.26(5)	Se(1)–Ru(3)–Ru(2)	56.69(6)
Se(1)–Ru(2)–Se(2)	80.74(6)	Ru(1)–Se(1)–Ru(3)	97.09(7)
Se(1)–Ru(2)–Ru(3)	55.85(5)	Ru(1)–Se(1)–Ru(2)	68.36(6)
Se(2)–Ru(2)–Ru(3)	55.45(5)	Ru(3)–Se(1)–Ru(2)	67.46(6)
Se(1)–Ru(2)–Ru(1)	55.38(5)	Ru(3)–Se(2)–Ru(1)	97.67(7)
Se(2)–Ru(2)–Ru(1)	55.07(5)	Ru(3)–Se(2)–Ru(2)	67.51(6)
Ru(3)–Ru(2)–Ru(1)	83.75(5)	Ru(1)–Se(2)–Ru(2)	68.36(6)

the bond distance Ru(1)–Ru(2) (2.91 Å) is significantly longer, whereas the distance Ru(3)–Ru(2) (2.76 Å) is shorter than those observed in cluster **3**, where the corresponding lengths (P)Ru(basal)–Ru(apical) are 2.80 and 2.83 Å. On the other hand, the Ru–Se interactions appear unaffected by P-substitution isomerism, the relevant distances in **2** being well comparable with the corresponding ones in **3**.

Finally, as regards cluster **3**, which is perfectly isostructural with the corresponding μ-dppe triiron species[7] and comparable to the $(CH_2)_3(PPh_2)_2$ ruthenium derivative,[9] there are two short intramolecular contacts between the two selenido ligands and the two methylene groups of the bridging diphosphine: H(8a)···Se(2) 2.97(1) Å, C(8)–H(8a)···Se(2) 124(1)°; H(9a)···Se(1) 2.93(1) Å, C(9)–H(9a)···Se(1) 123(1)°.

NMR and fluxionality

In order to gain an insight into the structures of these molecules in solution we have performed ^{1}H NMR investigations. At room temperature the proton pattern of **1** shows a featureless broad band in the cyclopentadienyl region, suggesting the onset of fluxional behaviour. At 258 K four singlets (*a*, *b*, *c*, *d*) are visible in the same region (Fig. 4a) indicating the equivalence of the two Cp rings. The relevant COSY spectrum (Fig. 4b) shows the scalar correlation pattern to be $a \longrightarrow d \longrightarrow b \longrightarrow c$, signals *a*, *c* being due to the α protons. The EXSY spectrum (Fig. 4c) discriminates the exchange (positive peaks) from the spatial connectivities (negative peaks, void circles). The positive cross peaks clearly indicate chemical exchange between *a* and *c* and between *b* and *d*. The negative cross peaks, correlating the aromatic phenyl region with the cyclopentadienyl region, denote the spatial proximity of the Ph *ortho*- with the Cp α-protons. The proton corresponding to *a* appears rather deshielded, in spite of its proximity to P, which in free dppf results in a shielding effect (α-H, δ 4.02 (q); β-H, δ 4.27 (t) in chloroform). Protons relevant to *b* and *c* exhibit normal shifts, *b* (β position) being less shielded than *c* (α position), as expected; the proton corresponding to *d* is unexpectedly shielded. Therefore, signal *a* should be attributed to proton 2 (see Scheme 3), its deshielding being possibly due, among other

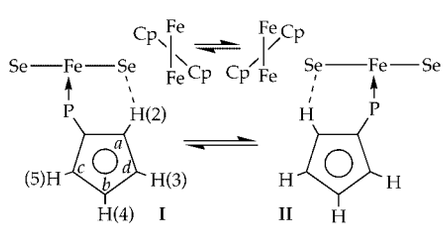

Scheme 3

things, to the C–H···Se interaction evidenced in the solid state structure; it follows that signals *b*, *c* and *d* correspond respectively to protons 4, 5 and 3. An inspection of the solid state structure reveals the reason (if we admit that the crystal structure is the preferred conformation in solution) because

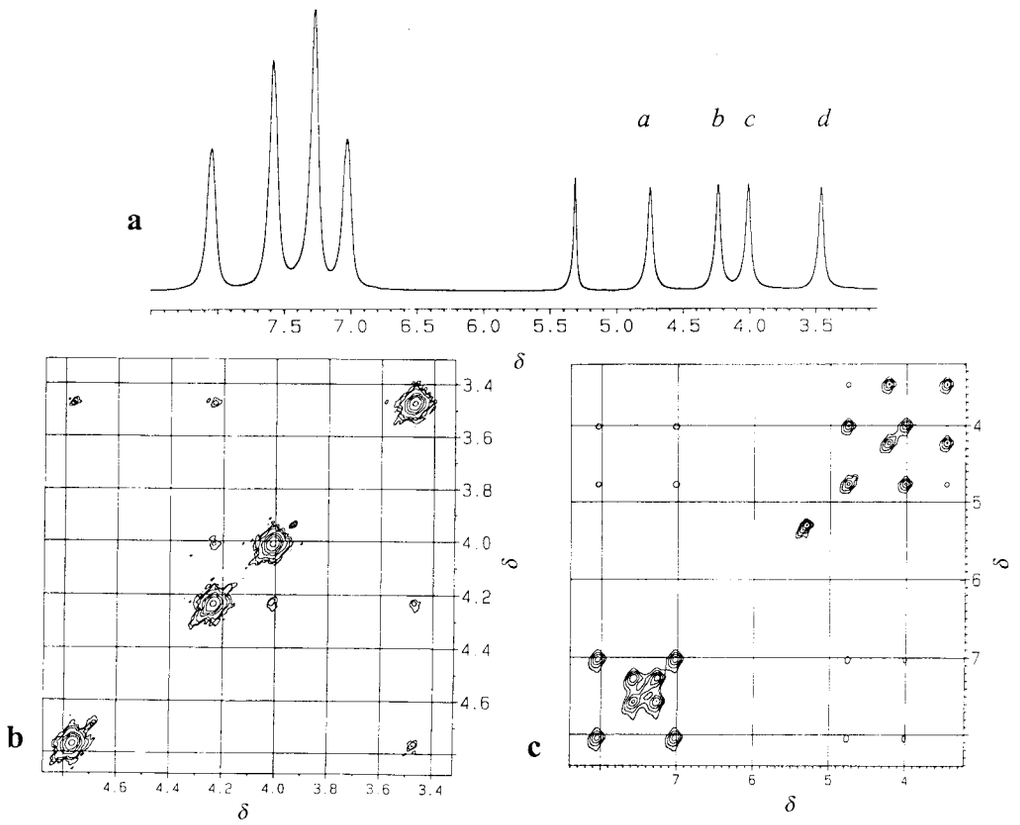

Fig. 4 The ^{1}H NMR spectra of **1**·CH_2Cl_2 at 258 K: (a) 1-D pattern; (b) 2-D COSY map of the Cp region; (c) 2-D EXSY map (*t* 0.5 s; negative peaks revealing spatial proximities are represented with only one level).

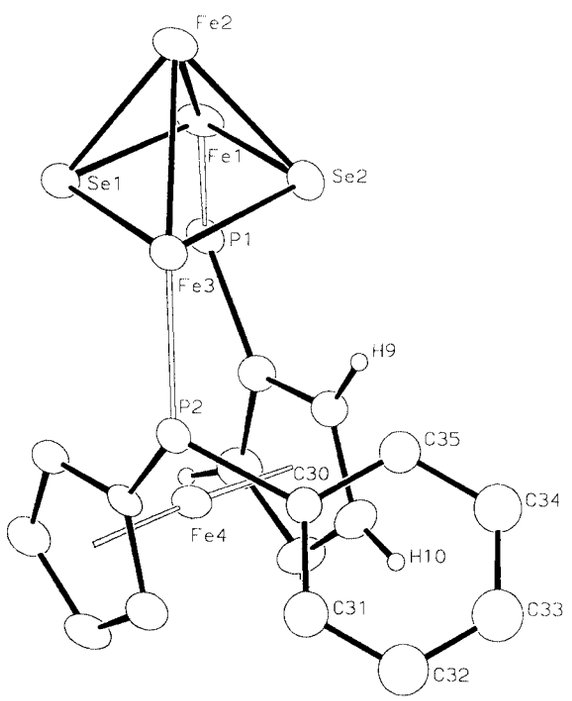

Fig. 5 Fragment of the solid state structure of compound **1** emphasizing the mutual position of proton H(10) (peak *d*) and ring C(30)–C(35).

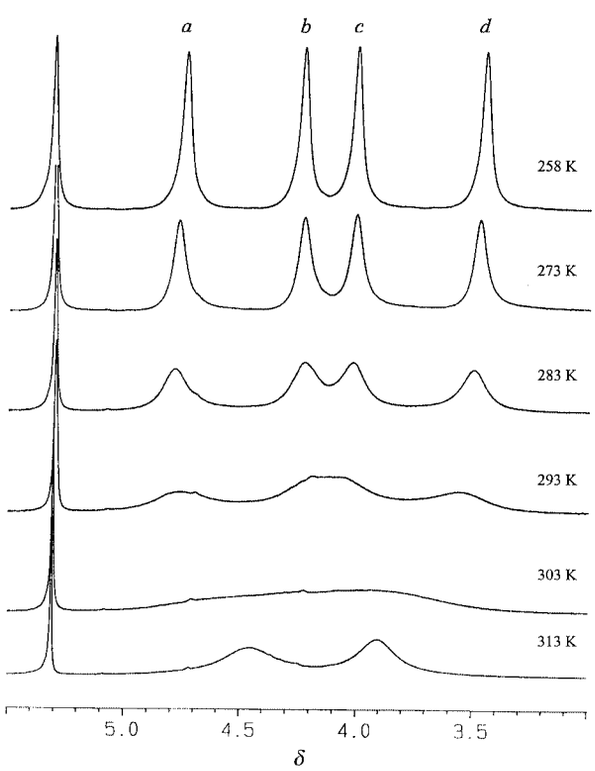

Fig. 6 The ^{1}H NMR spectra of compound **1**·CH_2Cl_2 in the Cp region recorded at different temperatures in the range 258–313 K.

proton 3 is shielded to a large extent: it lies just in the middle of the shielding cone of the phenyl ring C(30)–C(35) [Fig. 5; H(10)···C(35) 3.40(7) Å], being subjected to an estimated additional shielding of about 0.4 ppm.[24]

Having assigned the proton resonances, it is easy to understand the fluxional behaviour. Fig. 6 shows the variable temperature 1-D spectra of the Cp protons in the range 258–313 K. When the temperature is raised the four peaks broaden and coalesce (*a* with *c* and *b* with *d*), as evidenced by the EXSY map described above and confirmed by the ROESY spectrum, giving two peaks due to α and β protons respectively. This suggests that the fluxional behaviour consists in the concerted twisting

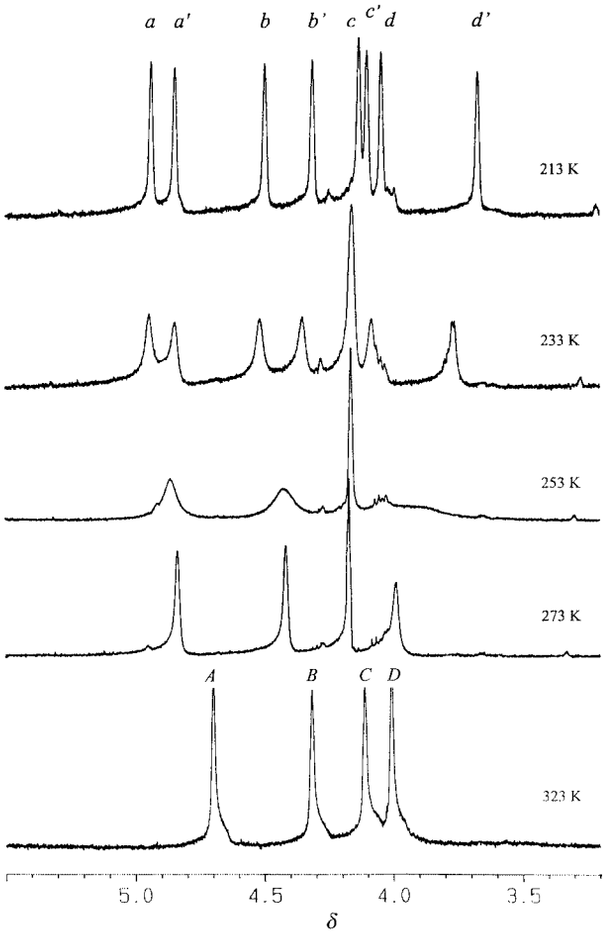

Fig. 7 The ^{1}H NMR spectra of compound **2** in the Cp region recorded at different temperatures in the range 213–323 K.

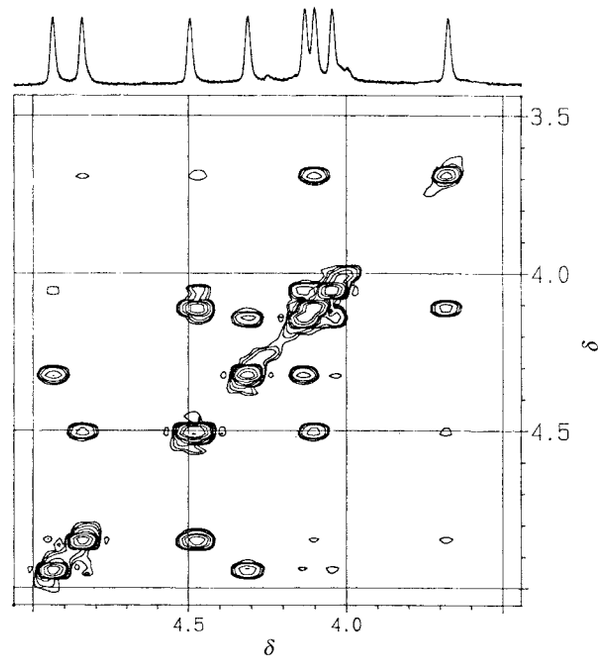

Fig. 8 The ^{1}H NMR COSY spectrum of compound **2** in the Cp region at 213 K.

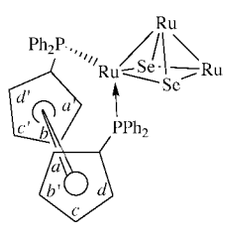

of the two equivalent rings around their axis equalizing protons 2 and 5 and 3 and 4, as shown in Scheme 3 ($\Delta G^{\ddagger}$ 58.2 kJ mol^{-1}, T_c 303 K). It is interesting that, whereas the co-ordinated P atoms maintain their axial position below the basal plane of the cluster core, the Cp–Fe–Cp axis is forced to oscillate under the Fe···Fe axis of the cluster. A similar rocking motion was observed in heteronuclear ruthenium–gold clusters[25,26] and in the dinuclear compound $[Re_2(\mu\text{-}OMe)_2(\mu\text{-}dppf)(CO)_6]$, where ring current effects were also considered to explain the Cp proton chemical shifts.[27] The approximate $\Delta G^{\ddagger}$ value observed for **1** appears rather higher than those found for the heteronuclear cluster described in ref. 26(*b*); this could be related with the presence in **1** of the C–H···Se interactions.

The dynamic behaviour of compound **2** is quite different. At room temperature the ^{1}H NMR spectrum exhibits four singlets (*A*, *B*, *C*, *D*) in the Cp zone (Fig. 7) indicating the equivalence of the two rings. At 213 K the two rings become inequivalent, the proton spectrum showing eight singlets *a*, *a*′, *b*, *b*′, *c*, *c*′, *d* and *d*′ (Fig. 7). The 297 K COSY map shows that the correlation pattern is $A \longrightarrow B \longrightarrow C \longrightarrow D$, *A* and *D* being the α protons. At 213 K the COSY map indicates two independent bond sequences, namely $a \longrightarrow b' \longrightarrow c \longrightarrow d$ and $a' \longrightarrow b \longrightarrow c' \longrightarrow d'$ (Fig. 8), *a*, *a*′, *d*, *d*′ corresponding to the α protons. The corresponding 2-D ROESY spectrum allows one to discriminate the exchange correlations from the dipolar ones due to spatial proximities: the pairs of signals *a*–*a*′, *b*–*b*′, *c*–*c*′ and *d*–*d*′, having the same diagonal phase, are clearly correlated by exchange. In fact they collapse respectively into *A*, *B*, *C* and *D* at room temperature. On the other hand, the signals *a*, *a*′, *d* and *d*′ showing through-space correlation between the relevant protons and phenyl rings are confirmed to correspond to Cp α protons. The reason for the large difference of chemical shift between the α-proton pairs *d*–*d*′ (particularly *d*′) and *a*–*a*′ should be ascribed again to the ring currents of the neighbouring phenyl rings. In fact, taking the solid state structure as a model of the frozen situation in solution, we observe that the Cp protons H(9) and H(17), bound to C(9) and C(17), approach the shielding cone of the rings C(36)–C(41) and C(24)–C(29) respectively [C(36)–H(9) 2.71, C(24)–H(17) 2.78 Å]. Consequently, they should be responsible for the peaks *d* and *d*′ (or *d*′ and *d*), protons H(12) and H(14) for *a* and *a*′ (or *a*′ and *a*). The proposed assignments for the frozen molecule are summarized above, taking into account that the two sequences of labels for the two rings could be exchanged.

Fig. 7 shows the proton spectra in the Cp region at different temperatures (213–323 K), emphasizing the fluxional behaviour of compound **2**, which should consist in the localized scrambling of the ligands around Ru(1), that is the exchange of the axial and equatorial positions between the two $Ph_2(C_5H_4)P$ moieties. This dynamic behaviour equalizes the two rings, but maintains unequal the four protons of each ring, indicating that rapid inversion at each P atom does not occur, otherwise the pairs of protons α and β would be time-averaged, resulting in a two-peak spectrum.[11a,28] In this regard the EXSY spectrum at room temperature indicates that this process is occurring at low rate, as the pairs of protons *A*–*D* and *B*–*C* are correlated by exchange.

The variable temperature ^{31}P NMR spectra afford additional evidence for the axial–equatorial scrambling. At 213 K the spectrum shows two unresolved doublets at δ 40.2 and 57.4 consistent with unsymmetrical co-ordination of the ligand. The lower field resonance should correspond to the axial phosphine group, being close to the value (δ 57.3) found for the dppe derivative **3**, where the bridging ligand occupies the two axial positions of the basal ruthenium atoms (Fig. 2). By raising the temperature the two resonances broaden, as expected, and

finally collapse in a single broad peak (δ 47.8) at 323 K ($\Delta G^{\ddagger}$ 50.2 kJ mol^{-1}, T_c 293 K). A similar dynamic behaviour was observed for an Ru_3S_2 *nido* cluster containing a different chelating diphosphine.[29]

Finally, as stated above, compound **3** exhibits a simple one-peak ^{31}P NMR spectrum, consistent with the solid state structure; correspondingly, the ^{77}Se spectrum shows a triplet at δ −231, significantly at lower frequency with respect to the corresponding dppm derivative (δ −121).[10b]

Acknowledgements

Financial support from Ministero dell'Università e della Ricerca Scientifica e Tecnologica (Rome, Cofin 98) is gratefully acknowledged.

References

1 L. C. Roof and J. W. Kolis, *Chem. Rev.*, 1993, **93**, 1037.
2 G. Hogarth, N. J. Taylor, A. J. Carty and A. Meyer, *J. Chem. Soc.*, *Chem. Commun.*, 1988, 834.
3 S. M. Stuczynski, Y.-U. Kwon and M. L. Steigerwald, *J. Organomet. Chem.*, 1993, **449**, 167.
4 W. Imhof and G. Huttner, *J. Organomet. Chem.*, 1993, **448**, 247.
5 P. Baistrocchi, D. Cauzzi, M. Lanfranchi, G. Predieri, A. Tiripicchio and M. Tiripicchio Camellini, *Inorg. Chim. Acta*, 1995, **235**, 173.
6 A. M. Z. Slawin, M. B. Smith and J. D. Woollins, *J. Chem. Soc.*, *Dalton Trans.*, 1997, 1877.
7 D. Cauzzi, C. Graiff, M. Lanfranchi, G. Predieri and A. Tiripicchio, *J. Organomet. Chem.*, 1997, **536**–**537**, 497.
8 Z.-G. Fang, Y.-S. Wen, R. K. L. Wong, S.-C. Ng, L.-K. Liu and T. S. A. Hor, *J. Cluster Sci.*, 1994, **5**, 327.
9 B. F. G. Johnson, T. M. Layer, J. Lewis, A. Martin and P. R. Raithby, *J. Organomet. Chem.*, 1992, **429**, C41.
10 (*a*) D. Cauzzi, C. Graiff, M. Lanfranchi, G. Predieri and A. Tiripicchio, *J. Chem. Soc.*, *Dalton Trans.*, 1995, 2321; (*b*) D. Cauzzi, C. Graiff, G. Predieri, A. Tiripicchio and C. Vignali, *J. Chem. Soc.*, *Dalton Trans.*, 1999, 237.
11 (*a*) K.-S. Gan and T. S. A. Hor, in *Ferrocenes*, eds. A. Togni and T. Hayashi, VCH, Weinheim, 1995, ch. 1; (*b*) P. Zanello, *ibid.*, ch. 7.
12 F. H. Allen and O. Kennard, *Chem. Des. Autom. News*, 1993, **8**, 31.
13 N. Walker and D. Stuart, *Acta Crystallogr.*, *Sect. A*, 1983, **39**, 158; F. Ugozzoli, *Comput. Chem.*, 1987, **11**, 109.
14 G. M. Sheldrick, SHELXS 86, Program for the Solution of Crystal Structures, Universität Göttingen, 1986.
15 G. M. Sheldrick, SHELX 97, Program for the refinement of crystal structures, University of Göttingen, 1997.
16 G. M. Sheldrick, SHELXL 93, Program for the refinement of crystal structures, University of Göttingen, 1993.
17 S. T. Chacon, W. R. Cullen, M. J. Bruce, O. B. Shawkataly, F. W. B. Einstein, R. H. Jones and A. C. Willis, *Can. J. Chem.*, 1990, **68**, 2001.
18 W. R. Cullen, S. J. Rettig and T. Zheng, *Organometallics*, 1992, **11**, 853.
19 A. J. Blake, A. Harrison, B. F. G. Johnson, E. J. L. McInnes, S. Parsons, D. S. Shephard and L. J. Yellowlees, *Organometallics*, 1995, **14**, 3160.
20 G. Rheinwald, H. Stoeckli-Evans and G. Süss-Fink, *J. Organomet. Chem.*, 1996, **512**, 27.
21 L. Pauling, *The Nature of the Chemical Bond*, Cornell University Press, Ithaca, NY, 1959.
22 M. I. Bruce, I. R. Butler, W. R. Cullen, G. A. Koutsantonis, M. R. Snow and E. R. T. Tiekink, *Aust. J. Chem.*, 1988, **41**, 963; A. Santos, J. Lopez, J. Montoya, P. Noheda, A. Romero and A. M. Echavarren, *Organometallics*, 1994, **13**, 3605; R. T. Hembre, J. S. McQueen and V. W. Day, *J. Am. Chem. Soc.*, 1996, **118**, 798; M. Sato and M. Asai, *J. Organomet. Chem.*, 1996, **508**, 121.
23 S. B. Jensen, S. J. Rodger and M. D. Spicer, *J. Organomet. Chem.*, 1998, **556**, 151.
24 H. Günther, *NMR Spectroscopy. An Introduction*, Wiley, Chichester, 1980, p. 380.
25 S. M. Draper, C. E. Housecroft and A. L. Rheingold, *J. Organomet. Chem.*, 1992, **435**, 9.
26 (*a*) I. D. Salter, V. Sik, S. A. Williams and T. Adatia, *Polyhedron*, 1995, **14**, 2803; (*b*) I. D. Salter, S. A. Williams and T. Adatia, *J. Chem. Soc.*, *Dalton Trans.*, 1996, 643.
27 S.-L. Lam, Y.-X. Cui, S. C. F. Au-Yeung, Y.-K. Yan and T. S. A. Hor, *Inorg. Chem.*, 1994, **33**, 2407.
28 C. Housecroft, S. M. Owen, P. R. Raithby and B. A. M. Shaykh, *Organometallics*, 1990, **9**, 1617.
29 H. Shen, S. G. Bott and M. G. Richmond, *Inorg. Chim. Acta*, 1996, **241**, 71.

Paper 9/04866I